PERGAMON

International Journal of Multiphase Flow 26 (2000) 1525–1543

International Journal of Multiphase Flow

www.elsevier.com/locate/ijmulflow

Pressure gradient and holdup in horizontal two-phase gas–liquid flows with low liquid loading

S. Badie, C.P. Hale, C.J. Lawrence, G.F. Hewitt*

Department of Chemical Engineering and Chemical Technology, Imperial College of Science, Technology and Medicine, Prince Consort Road, London SW7 2BY, UK

Received 1 August 1997; received in revised form 3 October 1999

Abstract

Pressure gradient and holdup data are presented for air–water and air–oil flows in a horizontal, 0.079 m diameter pipe. Addition of a very small liquid flow was found to result in a considerable increase in the pressure gradient compared with single phase gas flow. The pressure gradient and the holdup data were compared with predictions of the 'apparent rough surface' (ARS) and the 'double-circle' models. The ARS model generally gave better predictions for the holdup over the experimental range. Both models predicted the pressure gradient for air–water flows at high gas flowrates reasonably well. However, the predictions of both methods were unsatisfactory for air–water experiments at low gas flowrates and for air–oil experiments. Overall the ARS model was judged to be the more robust.

Keywords: Low liquid loading; Pressure gradient; Holdup; Two-phase flow

1. Introduction

Two phase gas–liquid flows are frequently encountered in petroleum pipeline systems, and the two phases may interact to produce dramatically different characteristics from those encountered in single phase flows. In many hydrocarbon pipelines, condensation of the gas phase, resulting from reduction in pressure and temperature along the line, leads to the formation of a small quantity of liquid which can cause a considerable increase in the pressure

* Corresponding author.

0301-9322/00/$ - see front matter
PII: S0301-9322(99)00102-0

gradient. The liquid flows partly as a layer on the pipe wall and partly as drops entrained in the gas phase. Here, we consider a horizontal pipe where the wall layer is asymmetric due to the influence of gravity. At low gas flowrates, the wall layer may cover only part of the pipe periphery but, at higher flowrates, the liquid can cover the whole of the periphery with the layer thickness being greater at the bottom than the top of the pipe; the latter case is horizontal annular flow. The former case has been referred to as partially annular flow or stratified-wavy flow. Knowledge of the amount of liquid present in the pipe and the distribution of the liquid phase is important in itself and especially in formulating models for such flows. This information is also important for modelling heat transfer and corrosion processes.

Attempts have been made to quantify the increased pressure drop in such flows compared with single phase gas flow. In the literature there are numerous empirical correlations (e.g. those of Hoogendoorn, 1959; Baroczy, 1965; Beggs and Brill, 1973; Friedel, 1979), but these are based on limited sets of data collected for specific experimental conditions. They are frequently found to be inadequate when applied to systems other than those on which they were originally based.

Alternatively, phenomenological models (McAdams et al., 1942; Lockhart and Martinelli, 1949; Taitel and Dukler, 1976; Hart et al., 1989; Chen et al., 1997; Vlachos et al., 1999) have been developed based on the interpretation of the dominant physical mechanisms of the process. However, these models generally rely on gross simplifying assumptions and empirical closure models, which tend to reduce their predictive capabilities. Major factors hindering modelling attempts include the inadequate representation of the interfacial interaction between the liquid film and the gas core region and an inability to determine the fraction of the liquid phase which is entrained as droplets.

In this work pressure gradient and holdup data collected from a general purpose multiphase flow facility (WASP) at Imperial College are presented and compared to predictions of models developed by Hart et al. (1989) and Chen et al. (1997). The WASP facility and the experimental method are described in Section 2. The two models of Hart et al. (1989) and Chen et al. (1997) are summarised in Section 3. Experimental results are then presented and compared with predictions of the models. Finally, conclusions are drawn on the relative performance of the two models in describing low holdup flows.

2. Experimental details

2.1. Experimental facility

The High Pressure WASP (Water, Air, Sand and Petroleum) rig located in the Chemical Engineering Department at Imperial College of Science, Technology and Medicine was used to perform the experiments described in this study. A schematic diagram of the facility is presented in Fig. 1.

The rig consists of a 37 m long, 78 mm internal diameter tubular stainless steel test section that can be used in the horizontal or slightly inclined ($+2^\circ$ to -2°) orientations. Gas and liquid phases are fed to the mixer at the entrance of the test section. The liquid phases used

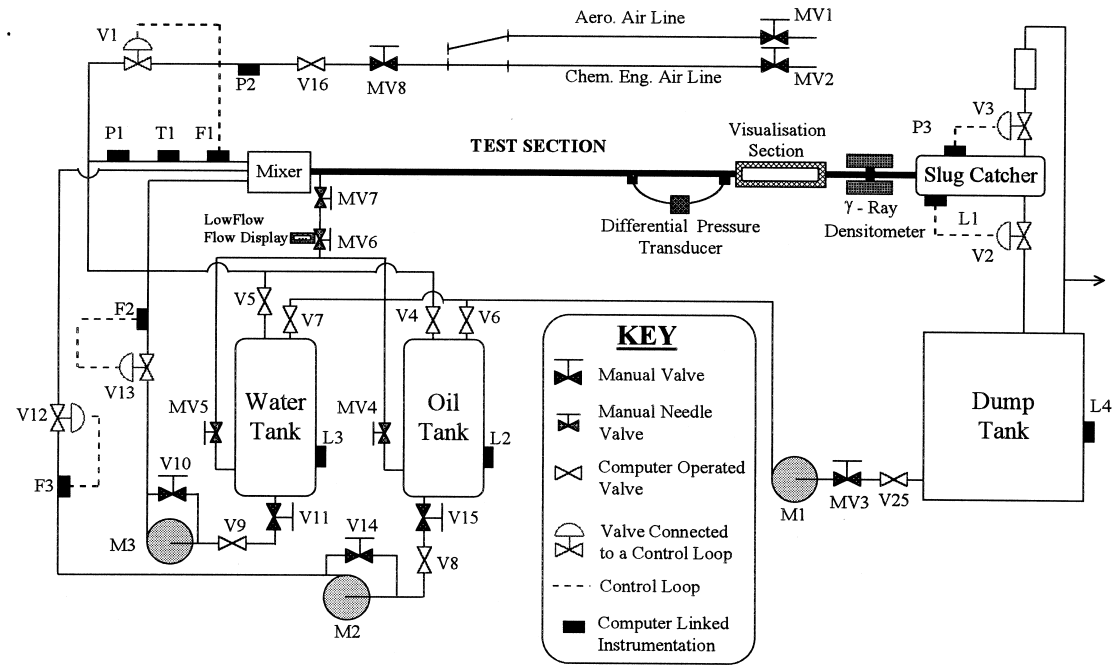

Fig. 1. The WASP facility.

were Shell Tellus 22 oil (density: 865 kg/m^3, viscosity: 40 MPa s, surface tension: 32 mN m^{-1} at 23.5°C) and water (density: 1000 kg/m^3, viscosity: 1 MPa s, surface tension: 37 mN m^{-1} at 23.5°C). The required liquid phase was fed to the testline from respective 5000 l storage tanks. The air supply was obtained from the adjacent Aeronautics Department's 65 m^3 high pressure tanks supplying air at 30 bar(g).

The WASP facility was operated in the 'blowdown' mode in which high pressure air from the supply tank flows through the test section and is released to atmosphere. The slug catcher acts as a primary separator of the gas and the liquid phases; the air is discharged through a silencer while the liquid phases are returned to the dump tank where (in the case where two liquid phases are employed) they are separated under the action of gravity before being returned to their respective feed tanks. In the present experiments, only one liquid phase (oil or water) was used.

The present tests were performed with the test section horizontal and with atmospheric pressure at the exit.

2.2. Measuring equipment

The superficial air velocity was measured using D and $D/2$ orifice plates built in accordance with BS1042 (1982). These are capable of determining the gas velocity to within ± 0.2 m s^{-1}. A Danfoss Mass3000 MassFlo flowmeter, specifically designed for measuring low liquid velocities (< 0.05 m/s) was used to determine the superficial velocities of either water or oil. This is

Table 1
Air–water experiments

Superficial gas velocity (m s^{-1})	Superficial liquid velocity (m s^{-1})	Number of runs
15	0.001–0.049	12
20	0.001–0.049	12
25	0.001–0.050	12

capable of determining the liquid velocity to within ± 0.0001 m s^{-1}. The pressure gradient was measured over a distance of 3.5 m using a Rosemount 3051 differential pressure transducer with an estimated accuracy of ± 5 Pa. The holdup measurements were carried out using the WASP gamma densitometer system designed and installed by Pan (1996). The measurements were carried out over a time sufficient to reduce the expected error to ± 0.0025 in the holdup value which ranged from 0.005–0.1.

2.3. Experimental

The experimental method used was identical for both air–water and air–oil runs. Prior to the experimental runs, the gamma densitometer was calibrated for each fluid, i.e. air, water and oil, with the pipe full of the fluid. During the experiments the superficial gas velocity was maintained at a set value. The superficial liquid velocity was adjusted and, once the system had reached steady state, the holdup was recorded. The densitometer control system was set to measure a full pipe scan, traversing horizontally between 15 positions across the pipe diameter. The system was set to remain at each position for 20 s and to acquire data during successive periods of 40 ms. During each run, the behaviour of the flow was recorded using a video camera at the transparent visualisation section. A separate experimental campaign was performed in a similar manner to obtain the pressure gradient data. Tables 1 and 2 show the superficial velocities used and the number of runs carried out in each range.

The range covered is represented by the shaded region in Fig. 2, which shows the flow regime map developed by Taitel and Dukler (1976).

Table 2
Air–oil experiments

Superficial gas velocity (m s^{-1})	Superficial liquid velocity (m s^{-1})	Number of runs
15	0.001–0.034	10
20	0.001–0.034	10
25	0.001–0.035	10

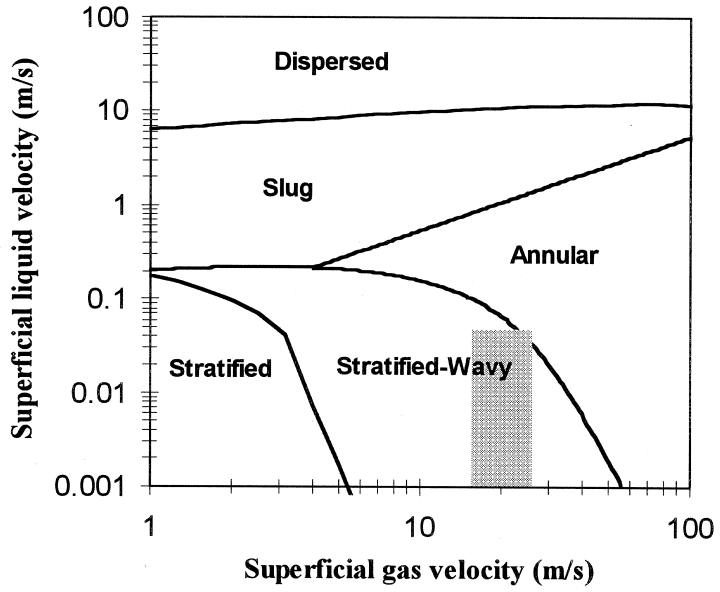

Fig. 2. Region of air–water flow data plotted on (Taitel and Dukler, 1976) flow pattern map (Note: a similar pattern is observed for air–oil data).

3. Models

3.1. The apparent rough surface (ARS) model

Pressure drop and holdup predictions were obtained using the ARS model, as summarised below (for further details see Hart et al., 1989). Here we present the model in terms of the mean gas and liquid velocities:

$$u_G = \frac{u_{G,S}}{(1-\varepsilon_L)}, \qquad u_L = \frac{u_{L,S}}{\varepsilon_L} \tag{1}$$

where $u_{G,S}$ and $u_{L,S}$ are the superficial velocities of the two phases and ε_L is the liquid phase holdup.

This model predicts the pressure drop in horizontal pipe flow at low liquid holdup by using a modified form of the gas phase pressure drop expression:

$$\Delta p_{TP} = 4 f_{TP}\left(\frac{L}{D}\right)\frac{1}{2}\rho_G u_G^2 \quad \text{for } u_G \gg u_i \tag{2}$$

where ρ_G is the gas density, L is the pipe length, D is the pipe diameter, u_i is the interface velocity and f_{TP} is a two-phase friction factor given by:

$$f_{TP} = (1-\phi) f_G + \phi f_i \tag{3}$$

where f_G and f_i are the gas phase and interfacial friction factors respectively, and ϕ is the fraction of the tube periphery wetted by the liquid layer. Thus, ϕ is given by:

$$\phi = \frac{\alpha}{2\pi} \tag{4}$$

where α is the angle subtended by the liquid layer at the pipe centre line (see Fig. 3).

In Eq. (3), the gas phase friction factor f_G is taken from Eck (1973) assuming a smooth pipe wall:

$$f_G = \frac{0.07725}{\left(\log_{10}\left(\frac{Re_G}{7}\right)\right)^2} \quad 2100 < Re_G < 10^8 \tag{5}$$

where Re_G is the gas phase Reynolds number given by $Re_G = Du_G\rho_G/\eta_G$ and η_G is the viscosity of the gas.

The interfacial friction factor f_i is calculated by representing the interface as a rough surface (Eck, 1973):

$$f_i = \frac{0.0625}{\left[\log_{10}\left(\frac{15}{Re_G} + \frac{k}{3.715D}\right)\right]^2} \tag{6}$$

where the surface roughness k is estimated to be a multiple of the mean film thickness, $\bar{h} = D\varepsilon_L/4\phi$:

$$k \approx 2.3\bar{h} \tag{7}$$

The fractional wetted perimeter ϕ is estimated using a correlation based on experimental data (Hart et al., 1989):

$$\phi = 0.52\varepsilon_L^{0.374} + 0.26Fr^{0.58} \tag{8}$$

The modified Froude number is defined as:

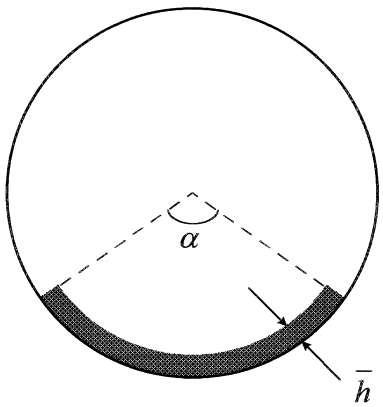

Fig. 3. Flow configuration used in the ARS model.

$$Fr = \frac{\rho_L u_L^2}{(\rho_L - \rho_G) g D} \tag{9}$$

where ρ_L is the liquid density and g is the acceleration due to gravity. The correlation for ϕ is simply truncated at $\phi = 1$.

Finally, Hart et al. used the force balance under steady state conditions to extend the correlation developed by Butterworth (1975). They derived the following equation decribing the liquid holdup ε_L:

$$\frac{\varepsilon_L}{1 - \varepsilon_L} = \frac{u_{L,S}}{u_{G,S}} \left[1 + \left(\frac{f_L \rho_L}{f_i \rho_G} \right)^{\frac{1}{2}} \right] \quad \varepsilon_L \leq 0.06 \tag{10}$$

where f_L is the liquid–wall friction factor.

The ratio of the liquid and the interfacial friction factors (f_L/f_i) was correlated (Hamersma and Hart, 1987) as a function of the liquid superficial Reynolds number, Re_{SL}, given by:

$$\frac{f_L}{f_i} = 108 Re_{SL}^{-0.726} \tag{11}$$

where $Re_{SL} = D u_{L,S} \rho_L / \eta_L$ and η_L is the liquid viscosity.

3.2. The double-circle model

A mechanistic model and a correlation for friction factor were proposed by Chen et al. (1997) to predict the liquid wetted wallfraction, liquid holdup and pressure drop for gas–liquid stratified-wavy flow in horizontal pipelines. This model is based on the flow geometry presented in Fig. 4.

Considering steady-state gas–liquid stratified-wavy flow in a horizontal pipe, neglecting droplet entrainment and assuming one-dimensional motion for each phase, the momentum balances for each phase may be written in the form:

$$-S_G \frac{dp}{dx} - \tau_{WG} P_G - \tau_i P_i = 0 \tag{12}$$

$$-S_L \frac{dp}{dx} - \tau_{WL} P_L + \tau_i P_i = 0 \tag{13}$$

where p is the pressure, x is the axial coordinate, S_G and S_L are the cross-sectional areas occupied by the gas and the liquid phase, P_G and P_L are the arc lengths of the pipe wall covered by the gas and the liquid, τ_{WG} and τ_{WL} are the shear stresses exerted at the pipe wall by the gas and liquid, τ_i is the interfacial shear stress and P_i is the interfacial arc length.

A single equation is obtained by eliminating the pressure gradient terms in Eqs. (12) and (13):

$$\tau_{WG} \frac{P_G}{S_G} - \tau_{WL} \frac{P_L}{S_L} + \tau_i P_i \left(\frac{1}{S_G} + \frac{1}{S_L} \right) = 0 \tag{14}$$

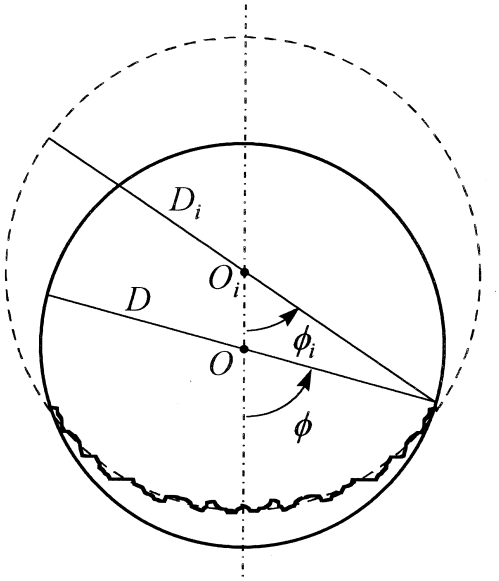

Fig. 4. Geometry of the 'double-circle' model.

The shear stress relationships used are:

$$\tau_{WG} = f_G \frac{\rho_G u_G^2}{2} \tag{15}$$

$$\tau_{WL} = f_L \frac{\rho_L u_L^2}{2} \tag{16}$$

$$\tau_i = f_i \frac{\rho_G (u_G - u_L)^2}{2} \tag{17}$$

Taitel and Dukler (1976) approach was adopted for calculating the gas and liquid friction factors:

$$f_G = C_G \left(\frac{D_G u_G}{\nu_G} \right)^{-m} \tag{18}$$

$$f_L = C_L \left(\frac{D_L u_L}{\nu_L} \right)^{-n} \tag{19}$$

where ν_G and ν_L are the kinematic viscosities of the gas and liquid phases respectively and D_G and D_L are the hydraulic diameters. If the flow is turbulent in both phases, the coefficients used are $C_G = C_L = 0.046$ and $m = n = 0.2$. However, for some of the flows considered here, the liquid Reynolds number is in the laminar range ($Re_L = D u_L \rho_L / \eta_L < 2100$) and the values used

are $C_L = 16$ and $n = 1$. The hydraulic diameters are evaluated by:

$$D_L = \frac{4S_L}{P_L}; \qquad D_G = \frac{4S_G}{P_G + P_i} \tag{20}$$

Chen et al. (1997) proposed the following correlation for the interfacial friction factor:

$$\frac{f_i}{f_G} = 1 + 3.75\left(\frac{\varepsilon_L}{\phi}\right)^{0.20}\left(\frac{u_{G,S}}{u_{G,S,t}} - 1\right)^{0.08} \tag{21}$$

where the transitional superficial gas velocity, $u_{G,S,t}$ is evaluated using the transition criterion proposed by Taitel and Dukler (1976):

$$u_{G,S,t} = \left(\frac{4\nu_L(\rho_L - \rho_G)g}{s\rho_G u_L}\right)^{0.5} \tag{22}$$

Andritsos and Hanratty (1987) proposed a value of 0.06 for the sheltering coefficient, s. The wetted wall fraction was calculated using the correlation (8) developed by Hart et al. (1989).

The relevant geometrical parameters in the double circle model (see Fig. 4) are expressed as:

$$P_G = (\pi - \theta)D, \quad P_L = \theta D, \quad P_i = \theta_i D_i \tag{23}$$

$$S_G = (1 - \varepsilon_L)\frac{\pi D^2}{4}, \qquad S_L = \varepsilon_L \frac{\pi D^2}{4} \tag{24}$$

where D and D_i are the diameters of the pipe and the circular interface respectively. Similarly, θ and θ_i are the angles subtended by the interface at centres O and O_i, respectively.

The following relationships were obtained from straightforward geometrical derivations:

$$D_i = D\frac{\sin\theta}{\sin\theta_i} \tag{25}$$

$$\theta_i = \left(\frac{\sin\theta_i}{\sin\theta}\right)^2\left(\theta + \frac{\sin^2\theta}{\tan\theta_i} - \frac{\sin 2\theta}{2} - \pi\varepsilon_L\right) \tag{26}$$

The subtended angle θ_i is obtained (for a given ε_L) using an iterative solution of Eq. (26) and the holdup ε_L is obtained using an outer iterative solution of Eq. (14).

4. Results and discussion

The experimental data are tabulated in Tables 3 and 4.

4.1. Holdup

Data for air–water experiments are compared with the predictions of Hart et al. (1989)

Table 3
Air–water experimental data

$u_{L,S}$ (m s^{-1})	$u_{G,S}$ (m s^{-1})	Pressure gradient (Pa m^{-1})	$u_{L,S}$ (m s^{-1})	$u_{G,S}$ (m s^{-1})	Holdup
0	15.2	30	0.001	15.18	0.008
0.003	14.75	22.54	0.002	15.02	0.010
0.007	14.61	26.43	0.005	15.37	0.014
0.011	14.55	22.25	0.010	15.09	0.022
0.014	14.56	31.57	0.015	15.01	0.028
0.018	14.51	34.04	0.020	15.04	0.033
0.022	14.69	43.48	0.025	15.02	0.039
0.025	14.63	46.97	0.030	15.45	0.041
0.029	14.63	45.47	0.035	15.29	0.046
0.033	14.56	45.60	0.040	15.06	0.051
0.034	14.54	43.79	0.045	14.76	0.055
0.038	14.56	41.77	0.049	15.4	0.056
0.038	14.61	51.86			
0.040	14.69	53.76			
0.042	14.50	56.49			
0.047	14.60	54.92			
0	20.3	54	0.001	20.39	0.005
0.001	19.96	47.15	0.002	20.07	0.010
0.002	19.79	49.13	0.005	19.89	0.010
0.005	19.54	60.23	0.011	19.69	0.019
0.010	20.10	76.65	0.015	20.23	0.022
0.015	20.47	84.90	0.020	20.22	0.025
0.020	20.23	86.45	0.025	19.68	0.029
0.025	20.07	89.11	0.030	19.8	0.032
0.030	19.53	91.95	0.035	20.1	0.035
0.035	19.94	100.67	0.040	20.2	0.039
0.037	20.10	100.97	0.045	20.12	0.041
0.045	19.60	115.72	0.050	20.09	0.043
0	24.53	90.25	0.001	24.77	0.005
0.001	25	93.92	0.003	25.25	0.008
0.005	24.53	115.60	0.005	24.6	0.010
0.011	24.73	138.40	0.010	25.27	0.016
0.015	24.66	148.23	0.015	24.77	0.018
0.020	24.68	169.02	0.020	25.02	0.021
0.025	24.53	177.17	0.025	24.85	0.024
0.030	24.8	190.90	0.030	24.9	0.027
0.035	24.75	204.28	0.035	25.03	0.028
0.040	25.34	215.22	0.040	25.12	0.031
0.046	25.25	228.52	0.045	25.03	0.034
			0.050	24.69	0.036

correlation in Fig. 5(a) and the same data are compared with Chen et al. (1997) model in Fig. 5(b). Similarly, data for air–oil experiments are compared with the predictions of the two methods in Fig. 6(a) and (b) respectively. The effect of the various system parameters is

Table 4
Air–oil experimental data

$u_{L,S}$ (m s^{-1})	$u_{G,S}$ (m s^{-1})	Pressure gradient (Pa m^{-1})	$u_{L,S}$ (m s^{-1})	$u_{G,S}$ (m s^{-1})	Holdup
0	15.2	30	0.001	15.01	0.021
0.001	14.98	64.93	0.003	15.36	0.029
0.003	14.69	76.68	0.005	15.05	0.040
0.005	14.55	83.87	0.008	15.09	0.052
0.008	15.23	101.38	0.010	14.86	0.064
0.010	14.96	103.95	0.015	14.99	0.083
0.015	14.95	114.19	0.020	15.37	0.091
0.020	14.72	124.07	0.025	15.36	0.095
0.024	15.14	137.14	0.030	14.88	0.106
0.029	15.34	147.34	0.034	14.99	0.110
0	20.3	54	0.001	19.58	0.016
0.002	20.27	117.57	0.003	19.91	0.024
0.003	20.06	131.51	0.005	19.59	0.033
0.005	19.68	145.35	0.008	20.45	0.041
0.008	20.23	165.88	0.010	19.7	0.050
0.010	20.34	172.98	0.015	20.02	0.062
0.015	20.12	190.37	0.020	19.75	0.071
0.020	20.01	209.03	0.025	19.75	0.080
0.026	20.1	230.99	0.030	20.05	0.083
			0.034	19.91	0.088
0	24.53	90.25	0.001	25.27	0.013
0.002	24.83	189.26	0.003	24.51	0.022
0.003	24.66	207.13	0.005	25.1	0.027
0.005	24.97	250.06	0.008	24.76	0.035
0.008	24.59	273.34	0.010	24.54	0.042
0.010	24.78	302.18	0.015	24.78	0.052
0.015	24.54	324.18	0.020	25.01	0.059
0.020	24.55	356.93	0.025	24.97	0.062
0.026	24.63	380.16	0.030	24.98	0.068
			0.035	24.94	0.068

discussed qualitatively in Section 4.1.1, while the comparisons with the correlation of Hart et al. (1989) and the model of Chen et al. (1997) are reviewed in Section 4.1.2.

4.1.1. Effect of system parameters on the holdup

4.1.1.1. Variation in $u_{L,S}$. An increase in the superficial liquid velocity (at constant gas velocity) leads to an increase in the holdup value. The rate of increase of holdup with $u_{L,S}$ is less than linear since the local liquid velocity also increases with increasing superficial liquid velocity. The overall effect is a faster moving liquid phase covering a greater proportion of the pipe cross-section and wetting a greater fraction of the pipe wall.

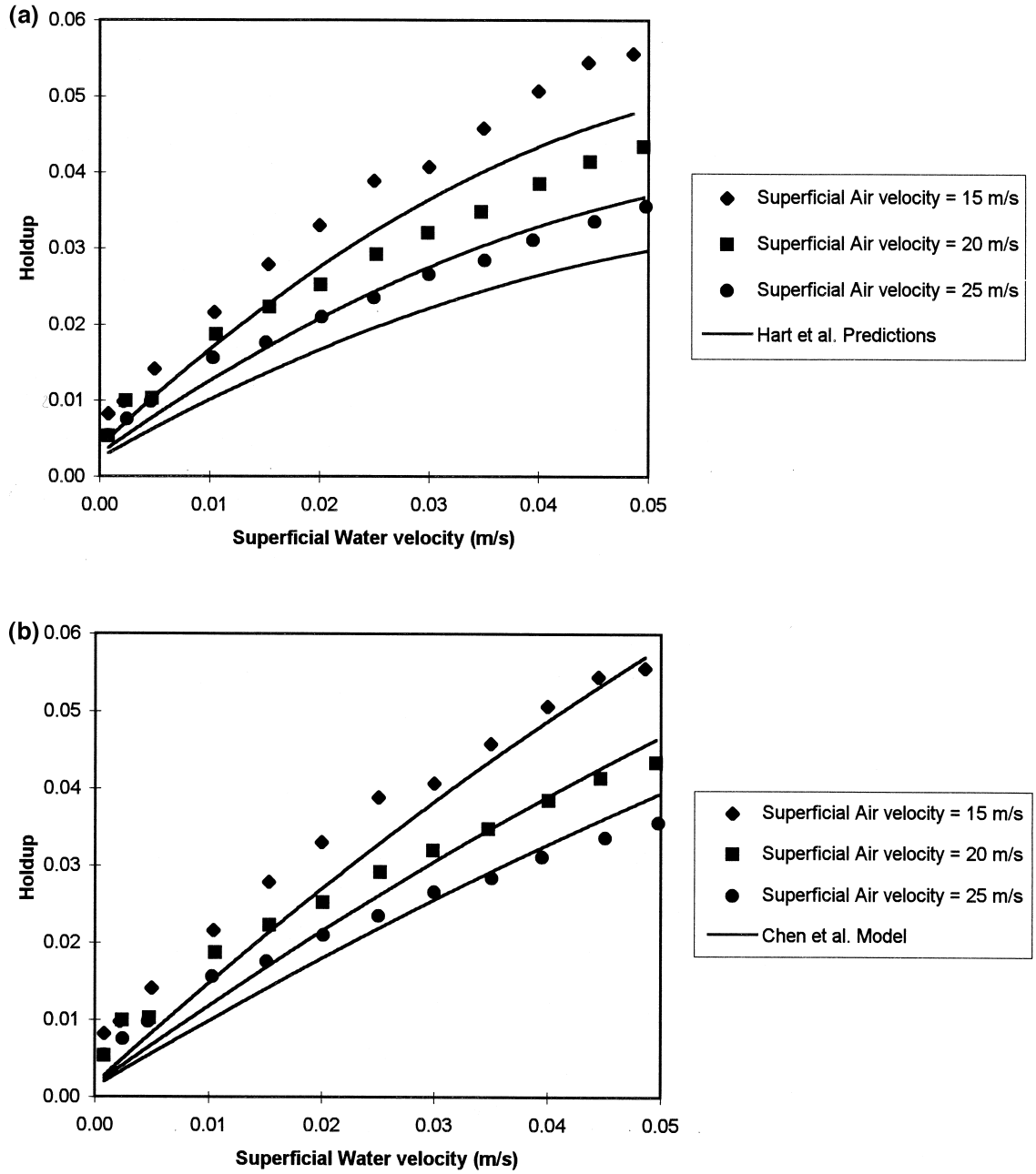

Fig. 5. (a) Air–water holdup data compared with predictions of the Hart et al. (1989) correlation. (b) Air–water holdup data compared with predictions of the Chen et al. (1997) model.

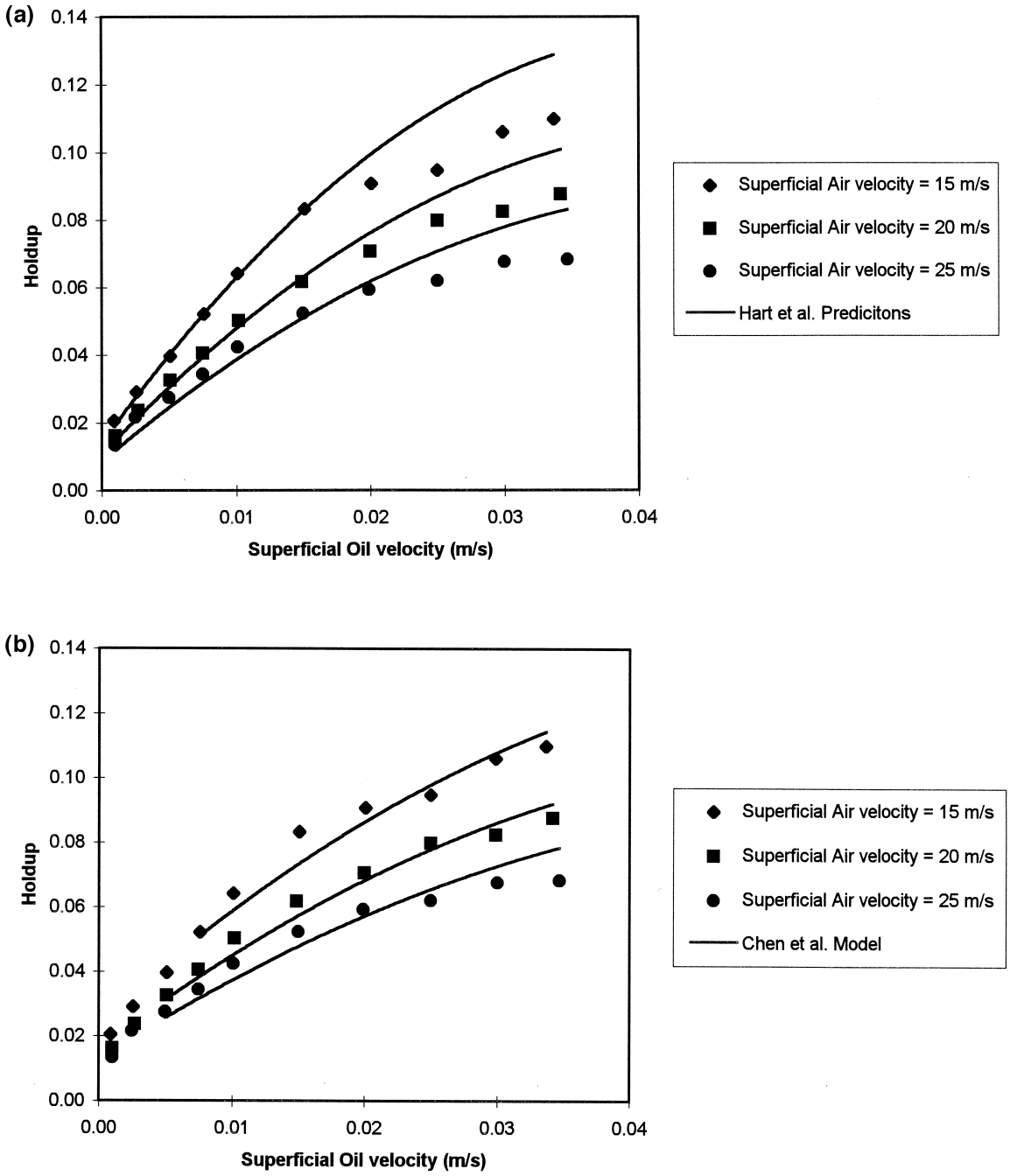

Fig. 6. (a) Air–oil holdup data compared with predictions of the Hart et al. (1989) correlation. (b) Air–oil holdup data compared with predictions of the Chen et al. (1997) model.

4.1.1.2. Variation in $u_{G,S}$. Lower holdup values were observed as the superficial gas velocity was increased at constant superficial liquid velocity. This decrease is due to the higher drag exerted on the liquid phase at the interface by the faster moving gas. The liquid moves faster, leaving a smaller amount of liquid in the pipe at any given time.

4.1.1.3. Liquid phase. The holdup values measured for the air–oil experiments were more than double the values for the corresponding air–water experiments. This is mainly due to the difference between the viscosities of the two liquid phases. For a given interfacial shear stress the actual liquid velocity is lower for the oil layer than for the water layer due to the higher viscosity of the oil phase. Consequently, the oil film moves more slowly than the water one under the same conditions, leading to a higher holdup value.

4.1.2. Comparisons of data with predictions

The 'double-circle' model of Chen et al. (1997) generally shows better agreement with the experimental data than the correlation developed by Hart et al. (1989). Both methods give satisfactory predictions for the air–water system, although the Chen et al. model performs better at higher and worse at lower superficial liquid velocities. The Hart et al. correlation agrees quite well with the air–oil data at low holdups and overpredicts at higher values. This is expected as the correlation was developed for holdup values below 0.06. The Chen et al. model produced good predictions for the air–oil data (based on laminar flow calculations for the liquid phase). However at low liquid superficial velocities, the model did not converge to a solution.

4.2. Pressure gradient

Data for air–water experiments are compared with the predictions of the ARS model in Fig. 7(a) and the same data are compared with the 'double-circle' model in Fig. 7(b). Similarly, data for air–oil experiments are compared with the predictions of the two methods in Fig. 8(a) and (b) respectively. The effects of the various system parameters are discussed qualitatively in Section 4.2.1, while the comparisons with the two models are reviewed in Section 4.2.2.

4.2.1. Effect of system parameters on the pressure gradient

4.2.1.1. Variation in $u_{L,S}$. An increase in the superficial liquid velocity (at constant gas velocity) leads to a substantial increase in the measured pressure drop (Figs. 7 and 8) even for very low liquid flowrates and especially at high gas flowrates. When the flowrate of the liquid is increased, a greater fraction of the (smooth) pipe wall is covered by a rough interface formed between the liquid and the gas, leading to an increased friction factor and pressure gradient.

4.2.1.2. Variation in $u_{G,S}$. An increase in the gas flowrate also leads to an increase in the measured pressure gradient. Most of this increase is simply due to the scaling of pressure drop with the square of the velocity (Eq. (2)). However, there is an additional increase that is due to the spreading of the liquid around a greater portion of the pipe perimeter. This increased area of 'rough surface' increases the pressure drop.

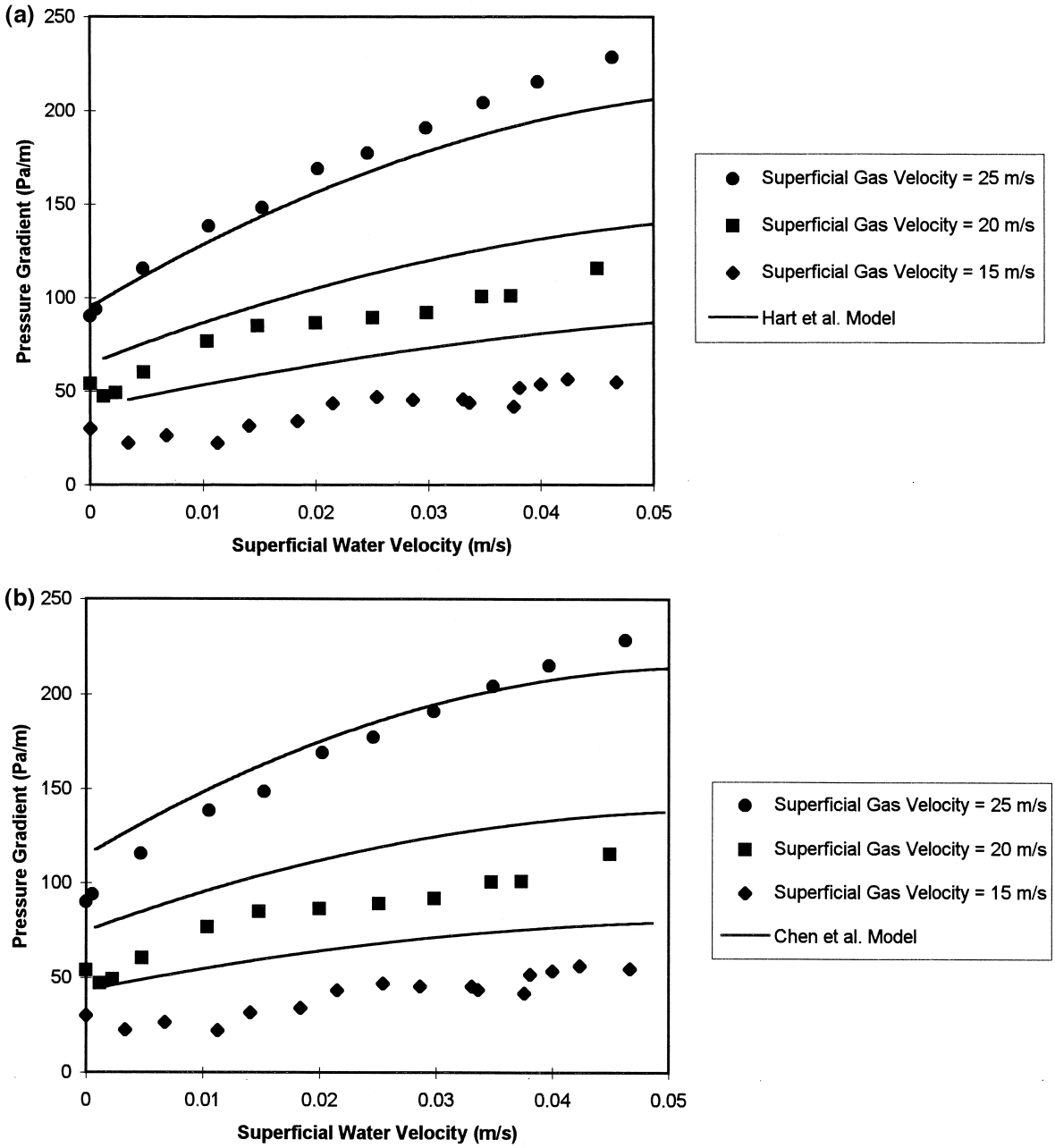

Fig. 7. (a) Air–water pressure gradient data compared with predictions of the Hart et al. (1989) model. (b) Air–water pressure gradient data compared with predictions of the Chen et al. (1997) model.

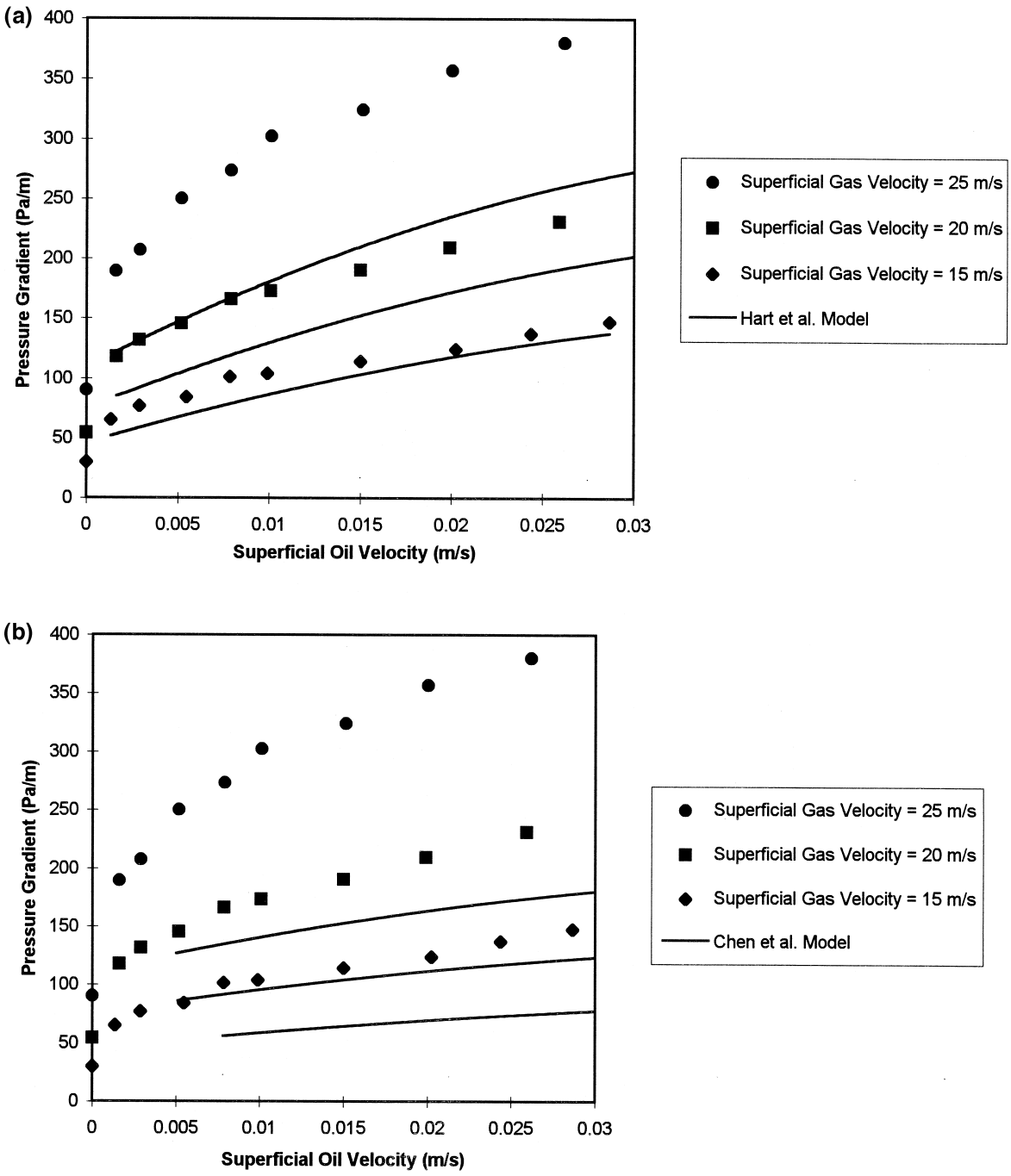

Fig. 8. (a) Air–oil pressure gradient data compared with predictions of the Hart et al. (1989) model. (b) Air–oil pressure gradient data compared with predictions of the Chen et al. (1997) model.

4.2.1.3. Liquid phase. The runs carried out using oil as the liquid phase produced a much greater increase in pressure drop for a given superficial liquid velocity than those carried out with the water. Experimental observations suggest that the oil formed a rougher interface with the gas phase compared with the water. Furthermore, in the oil runs, in addition to the main liquid region a very thin liquid layer was seen moving slowly along the upper surface of the pipe. This thin film would certainly increase the wall friction, adding to the pressure drop caused by the thicker liquid layer at the bottom of the pipe.

4.2.2. Comparisons of data with predictions

Both the Hart et al. (1989) (ARS) and the Chen et al. (1997) (double-circle) models overpredicted the pressure gradient for the air–water flows at lower gas flowrates. The ARS model slightly underpredicted the pressure gradient at the highest gas flowrate, with the discrepancy increasing with increasing liquid flowrate. At the same gas flowrate, the 'double-circle' model overpredicted the pressure gradient at low liquid flowrates while at higher liquid flowrates it underpredicted the pressure gradient, with the discrepancy increasing with increasing liquid flowrate.

For the air–oil tests, both models consistently underpredicted the pressure gradient, with the discrepancy increasing with increasing gas flowrate. However, the ARS model gave reasonable agreement with the experimental data at lower gas flowrates and generally gave better predictions than the 'double-circle' model over the experimental range.

The overprediction of the pressure gradient for air–water flows at low gas velocities probably results from the flow being closer to stratified than the partially annular geometry of the models. The better agreement at high gas velocities probably signifies that the appropriate flow regime for the models has been entered.

The gross underprediction of the pressure gradient for the air–oil flows shows that neither model adequately scales the effect of the physical properties. Hoogendoorn (1959) incorporated the effect of liquid viscosity in the empirical pressure gradient correlation that he developed for stratified and wave flow. In his experiments, he used gas oil (viscosity: 2.4 MPa s), spindle oil (viscosity: 20.8 MPa s) and water and also observed a large effect of viscosity on pressure gradient and holdup. However, his correlation performs significantly worse than either the Hart et al. (1989) or the Chen et al. (1997) methods.

5. Conclusion

Two-phase gas–liquid pressure gradient measurements obtained on the Imperial College WASP facility demonstrate that the addition of extremely low liquid flows results in a considerable increase in the pressure gradient compared to values measured for single phase gas flow. Comparisons with the ARS model of Hart et al. (1989) and the 'double-circle' model of Chen et al. (1997) show that both models agree reasonably well with the air–water data at the higher gas flowrates. The models overpredict the pressure gradient for air–water flows with low gas velocity, probably because a more stratified type of flow is occurring. The models underpredict the pressure gradient for the air–oil flows over the whole range. The underprediction of the air–oil data appears to arise from a failure of the models to capture the

greater propensity of the oil (40 MPa s) to spread around the tube surface. Over the entire experimental range, the ARS model performed better.

Holdup measurements were also made and compared with the correlation of Hart et al. (1989) and the model of Chen et al. (1997). The 'double-circle' model of Chen et al. (1997) generally showed better agreement with the experimental data than the correlation developed by Hart et al. (1989). However, for air–oil flows, within the range specified by the authors, the correlation developed by Hart et al. (1989) gave better agreement.

The somewhat better performance of the holdup correlation (Hart et al., 1989) compared to the model (Chen et al., 1997) is interesting since system dependence is normally associated with correlations rather than phenomenological models. This highlights a rather serious difficulty associated with phenomenological modelling. To obtain closure and complete the model, correlations are often introduced that are system dependent. Such models are then found to be inadequate when applied to systems other than those for which they were originally 'tuned'. If not worse, they are no better than straightforward correlations, as demonstrated in this study. The pressure gradient in the flows studied here is strongly dependent on holdup. Hence a good method for predicting the holdup is necessary, although not sufficient, for developing a reliable phenomenological model for pressure drop. The Chen et al. model is an example of the latter case; although the air–oil holdup was well predicted the pressure gradient was poorly predicted. Tuning this model to predict the pressure gradient more satisfactorily would probably have adverse effects on the holdup predictions.

Acknowledgements

The authors would like to thank the WASP Consortium for the financial support of this work. In addition, gratitude is extended to S.A. Fisher for invaluable discussions and to E. Jorisi for experimental assistance.

References

Andritsos, N., Hanratty, T.J., 1987. Interfacial instabilities for horizontal gas–liquid flows in pipelines. Int. Journal of Multiphase Flow 13, 583–603.

Baroczy, C.J., 1965. A systematic correlation for two phase pressure drop. Chemical Engineering Progress Symposium Series 62, 232–249.

Beggs, H.D., Brill, J.P., 1973. A study of two phase flow in inclined pipes. Journal of Petroleum Technology 255, 607–617.

Butterworth, D., 1975. A comparison of some void-fraction relationships for co-current gas–liquid flow. Int. Journal of Multiphase Flow 1, 845–850.

Chen, X.T., Cai, X.D., Brill, J.P., 1997. Gas–liquid stratified-wavy flow in horizontal pipelines. Journal of Energy Resources Technology 119, 209–216.

Eck, B., 1973. Technische Stromunglehre. Springer, New York.

Friedel, L., 1979. Improved friction pressure drop correlations for horizontal and vertical two phase pipe flow. In: European Two Phase Flow Group Meeting E2, Ispra, Italy, June 3–8.

Hamersma, P.J., Hart, J., 1987. A pressure drop correlation for gas/liquid pipe flow with a small liquid holdup. Chemical Engineering Science 42, 1187–1196.

Hart, J., Hamersma, P.J., Fortuin, J.M.H., 1989. Correlations predicting frictional pressure drop and liquid holdup during horizontal gas liquid pipe flow with a small liquid holdup. Int. Journal of Multiphase Flow 15, 947–964.

Hoogendoorn, C.J., 1959. Gas–liquid flow in horizontal pipes. Chemical Engineering Science 9, 205–217.

Lockhart, R.W., Martinelli, R.C., 1949. Proposed correlation of data for isothermal two-phase, two-component flow in pipes. Chemical Engineering Progress 45, 39–48.

McAdams, W.H., Woods, W.K., Heroman, L.C., 1942. Vapourisation inside horizontal tubes. Part II: benzene–oil mixtures. Transaction of ASME 64, 193–200.

Pan, L., 1996. High pressure three-phase (gas/liquid/liquid) flow. Ph.D. thesis, University of London.

Taitel, Y., Dukler, A.E., 1976. A model for predicting flow regime transitions in horizontal and near horizontal gas–liquid flows. AIChE Journal 22, 47–55.

Vlachos, N.A., Paras, S.A., Karabelas, A.J., 1999. Prediction of holdup, axial pressure gradient and wall shear stress in wavy stratified and stratified/atomisation gas/liquid flow. Int. Journal of Multiphase Flow 25, 365–376.